The 9th European Congress on Computational Methods in Applied Sciences and Engineering
ECCOMAS Congress 2024
3 – 7 June 2024, Lisboa, Portugal

PERFORMANCE ANALYSIS OF AN ORGAN-ON-CHIP DEVICE THROUGH CFD SIMULATIONS

ELENA FASIL[1], RACHELE LAMIONI[2], ALESSANDRO MARIOTTI[2], ELISABETTA BRUNAZZI[2], CHIARA GALLETTI[2], AND SERENA DANTI[2]

[1] Dipartimento di Ricerca Traslazionale e Nuove Tecnologie in Medicina e Chirurgia, Università di Pisa, via Savi 10, 56126 Pisa, Italy
[1] Dipartimento di Ingegneria Civile ed Industriale, Università di Pisa, Largo Lucio Lazzarino 2, 56122 Pisa, Italy

Keywords: *Organ-on-chip, cell culture, performance analysis, Computational Fluid Dynamics*

Summary: Three-dimensional *in-vitro* cell cultures replicate the microenvironment in which cells live. Among cell culture techniques, organ-on-chips enhance cell proliferation and expression, and in some cases replicate the physiological stimuli that cells perceive in native tissues. In this work, Computational Fluid Dynamics (CFD) simulations have been carried out to analyze the performance of an organ-on-chip platform, ensuring optimal conditions for cell culture and therapy perfusion under controlled parameters. We numerically evaluate the flow patterns within the chip to verify if they facilitate efficient and time-controlled turnover of biological substances, thereby maximizing cell viability and proliferation. Furthermore, we demonstrate that by precisely controlling the flow rates of culture media and therapy substances entering the organ-on-chip, it is possible to selectively target cells for therapy, allowing a direct comparison of the viability of treated versus untreated cells on the same scaffold.

1. INTRODUCTION

The investigation of tumors and personalized therapies is very challenging since it requires to replicate tissue-like microenvironments, in which cell behavior, morphology, interactions, and potential pharmacological therapies can be studied. Despite the still crucial role played by animal models in therapy testing, the intrinsic complexity of these models, the differences in drug metabolism between animals and humans, and some ethical concerns limit the accuracy of these models. Nowadays, traditional static cancer-cell cultures (usually called two-dimensional *in-vitro* cultures) don't allow to reproduce biomechanical stimuli and are subjected to nutrient depletion and toxic waste buildup. On the contrary, dynamic cancer-cell cultures (three-dimensional *in-vitro* cultures) use porous biomaterial scaffolds for cancer-cell growth and provide proper stimuli to improve the reliability of drug testing and personalized treatment assessment [1].

Among the dynamic cancer-cell cultures, organ-on-chip systems are a promising alternative to static *in-vitro* cell cultures and animal testing. Organs on chip may replicate various biological and pathological processes typical of the human body thanks to bioengineering and microfluidic optimization of the devices. Moreover, these chips are characterized by micrometric channels

and micrometric chambers equipped with scaffolds that can support mono- and multi-cell cultures, mimicking the native biological microenvironment. These microstructures are fed by a continuous laminar fluid flow that creates a dynamic system observable in real time, reproducing physiological stimuli through continuous medium perfusion and controlled mechanical stresses [2]. The microfluidic system within the device enables precise control and manipulation of the microenvironment in which cells live. In particular, the geometry of the device (culture chamber, scaffold porosity, and inlet/outlet microchannels) and fluid dynamic parameters (flow rates, mixture properties, …) significantly impact cell morphology, adhesion, and proliferation [3, 4, 5]. Computational Fluid Dynamic (CFD) studies play a fundamental role in analyzing the performance and in optimizing the design of the chip. Indeed, the simulations of the flow patterns inside the chips allow to improve the homogeneity of cell cultures and to promote cell proliferation and expression through the creation of uniformly perfused systems for nutrients and the elimination of waste substances [6]. Moreover, fluid dynamic studies allow the control of therapy perfusion by selecting treated and not-treated cells on the scaffold within the culture chamber of the organ on chip.

In this study, CFD simulations are utilized to assess the performance of an organ-on-chip device designed for cancer cell cultures. The focus is on evaluating whether the device's geometry and the selected flow rates efficiently and homogeneously distribute and remove biological substances, thereby ensuring optimal cell viability. Specifically, our goals are: (i) to achieve uniform nutrient perfusion across all cells residing on the scaffold within the culture chamber, with a controlled nutrient residence time, (ii) to ensure consistent and efficient waste elimination for all cancer cells, and (iii) to accurately control therapy perfusion by selectively targeting treated and untreated cells on the scaffold. The CFD simulations of the fluid flow within the chip play a fundamental role in verifying these objectives, ensuring that all seeded cells experience physiological conditions and appropriate mechanical stimuli.

2. GEOMETRY DEFINITION AND SIMULATION SET-UP

The geometry of the investigated organ on chip is shown in Fig. 1. It is an open system including a cell-culture chamber and two couples of inlet/outlet channels.
The cell-culture chamber is equipped with a spongy scaffold colonized by cells. The cell-culture chamber has a rectangular base with B_3=7 mm and W_3=10 mm, vertically extruded for H_3=2 mm. The spongy scaffold is modeled as a homogeneous porous zone in the simulations. The two inlet channels are filled through two syringe pumps and the outlet channels flow into two reservoirs. The channel C_1 is connected to the cell-culture chamber for nutrient supply, and it exits from the chamber to provide waste elimination. Drug or immune cell transport in the chamber is obtained through the channel C_2, which is switched on only during therapy. C_1 and C_2 channels have a rectangular cross-section with W_2=500 μm and H_2=400 μm. The channels are on the bottom side of the organ-on-chip platform. The connection between the channels and the syringe pumps is obtained with circular vertical channels with diameter P_1=0.75 mm and height H_1= 3 mm.

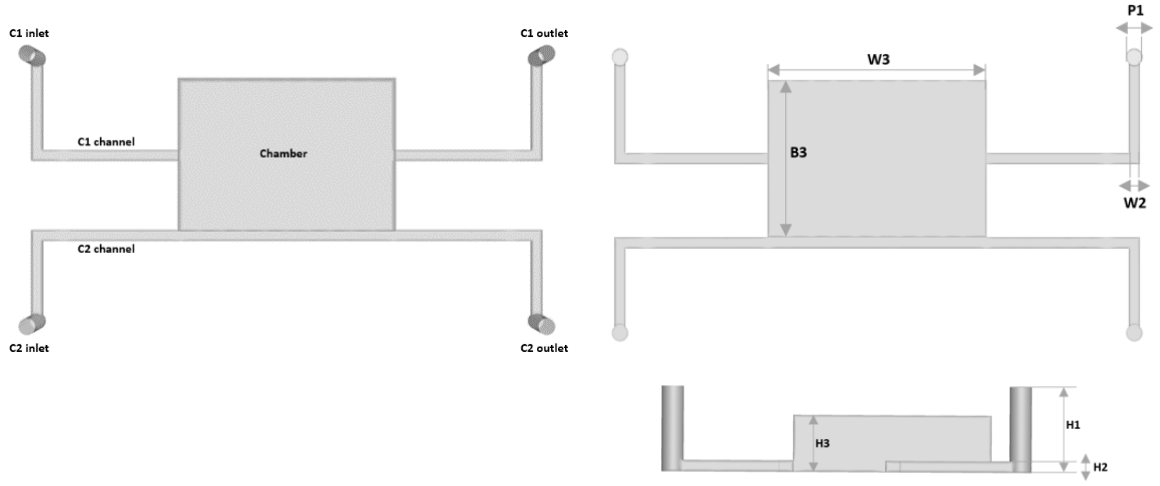

Figure 1: Sketch of the organ-on-chip geometry.

The incompressible steady-state laminar version of the Navier-stokes equations is solved for the microfluidic system. The equations are:

$$\nabla \cdot \vec{v} = 0$$

$$(\vec{v} \cdot \nabla)\vec{v} = -\frac{1}{\rho}\nabla p + \nu\nabla^2\vec{v} + \vec{g}$$

where $\vec{v} = (u, v, w)$ is the velocity vector, p is the pressure, ρ is the density of the fluid, ν is the kinematic viscosity of the fluid, and $\vec{g}$ is the gravity vector. Laminar hypothesis is justified by the fact that the Reynolds number, based on the bulk velocity and the hydraulic dimeter of the channels, is $Re \leq 10^{-3}$ for all the considered operating conditions.

The flow inside the microfluidic system is solved by using a commercial finite-volume code. The SIMPLE algorithm is selected for pressure-velocity coupling together with second order accurate schemes. The computational domain is discretized using an unstructured tetrahedral grid. We carried out grid sensitivity studies (not shown here for the sake of brevity) and grid independence is reached for a grid having $2 \cdot 10^6$ nodes. As for the boundary conditions, flow rates are imposed at the inlets of channels C_1 and C_2 and at the outlet of channel C_2, whereas reference pressure is set at the outlet of channel C_1. When therapy is not perfused, only channel C_1 has a non-zero flow rate. On the contrary, both channels have non-zero flow rates when therapy is given. No-slip boundary conditions are always used for channel and chamber walls. The working fluid is the RPMI-10% FBS cell culture medium, having density ρ = 999 kg/m^3 and viscosity μ = 0.9 mPa·s [7]. The culture medium is treated as a Newtonian fluid. The variation of the fluid properties with the adding of drugs to the culture medium is negligible.

In CFD simulations we do not consider the 3D sponge scaffold structure placed in the cell-culture chamber. The cell-culture chamber is modeled as a porous medium, thus following Darcy's law:

$$\mathrm{u} = -\frac{K}{\mu}\nabla p$$

$$K = \frac{d_p^2\,\varepsilon^3}{180\,(1-\varepsilon)^2}$$

where K represents the material permeability, μ denotes the dynamic viscosity of the fluid, d_p is the averaged diameter of the pores in the sponge scaffold (100 μm for the present application), and ε is the material porosity. The porous region in the chamber is defined based on the properties of the scaffold placed inside the chamber. The viscous resistance was calculated using the following formula:

$$\frac{1}{\alpha} = \frac{A}{\varphi^2 d_p^2}\mathrm{x}\frac{(1-\varepsilon)^2}{\varepsilon^3}$$

where φ is the sphericity of the pores of the sponge scaffold, assumed to be 1, and A is set equal to 150, considering the random, isotropic, and unstructured nature of the pores. The sensitivity to the scaffold porosity is analyzed to investigate its impact both on the nutrient and drug perfusion within the chamber and on the residence times of the biological substances injected. Three different values of porosity have been considered in this work, viz. 85%, 90%, and 95%.

Key quantities of interest in the CFD simulations are: (i) flow homogeneity within the cell culture chamber, to ensure uniform nutrient supply and waste removal for all the cells, while preventing stagnant or recirculating zones, and (ii) controlled drug therapy injection to a specific area of the cell culture chamber. Additionally, it is crucial to assess the residence time of nutrients, waste, and drugs in the cell culture chamber, which should be approximately 2 days for nutrient absorption, 2.5 days for waste elimination, and 1 day for complete drug assimilation, based on conventional *in-vitro* static cell culture benchmarks. Narrow residence-time distributions in the chip indicate homogeneous culture conditions, which can enhance cell viability. To evaluate these quantities of interest, we compute the velocity field by solving the Navier-Stokes equations in the CFD solver. Subsequently, we inject and track massless particles (one-way coupled) to calculate their residence time distribution within the organ-on-chip. Particles are introduced from the inlet of the C_1 channel to assess nutrient supply, from the volume of the cell culture chamber to evaluate waste elimination performance, and from the inlet of the C_2 channel to assess drug therapy.

The test matrixes for the numerical simulations without and with drug release are presented in Tables 1 and 2. The reference configurations are case 1 (without the drug release) and case 1d (with therapy infusion). Once assessed the performance of the reference configuration, simulations have been conducted to examine the effect of scaffold porosity (ranging from 85% to 95%) on flow patterns in the cell culture chamber and on the characteristic residence times

(cases 1, 2, and 3 and cases 1d, 2d, and 3d). Subsequently, we investigated the impact of the velocity ratio v_1/v_2 between channels C_1 and C_2 on the selection of the region of the cell culture chamber subjected to drug therapy. Three scenarios were considered: $v_1 = v_2$, $v_1/v_2 = 1/10$, and $v_1 = 0$ (cases 1d, 4d and 5d).

Table 1: Test matrix of the numerical simulations of the organ on chip operating without drug release

	Scaffold porosity	Velocity v_1	Velocity v_2
Case 1	90%	0.0015 mm/s	0 mm/s
Case 2	85%	0.0015 mm/s	0 mm/s
Case 3	95%	0.0015 mm/s	0 mm/s

Table 2: Test matrix of the numerical simulations of the organ on chip operating with drug release

	Scaffold porosity	v_1/v_2 ratio	Velocity v_1	Velocity v_2
Case 1d	90%	1/10	0.00027 mm/s	0.0027 mm/s
Case 2d	85%	1/10	0.00027 mm/s	0.0027 mm/s
Case 3d	95%	1/10	0.00027 mm/s	0.0027 mm/s
Case 4d	90%	0/1	0 mm/s	0.00297 mm/s
Case 5d	90%	1/1	0.001485 mm/s	0.001485 mm/s

3. RESULTS AND DISCUSSION

3.1 Analysis of the performance of the reference configuration

We first considered Case 1, with a scaffold porosity of 90% and without drug release. The trajectories for nutrient supply and waste elimination are shown in Fig. 2, and the corresponding residence times are presented in Fig. 3 as Probability Density Functions (PDFs). Nutrients entering the cell culture chamber from channel C_1 spread out, occupying almost the entire volume of the cell culture chamber. However, there are small regions near the corners of the chamber where nutrients do not reach due to the presence of small stagnant zones. By properly selecting the velocity v_1, it is possible to achieve an average nutrient residence time of 2 days (left panel of Fig. 3). However, due to the varying lengths of nutrient trajectories within the cell culture chamber, the PDF of nutrient residence times is broad, ranging from about 1.5 days to more than 3 days (see the tail of the PDF distribution in the left panel of Fig. 3). The waste elimination time shows an even broader distribution (see the right panel of Fig. 3). From the waste trajectories shown in the right panel of Fig. 2, the waste produced by cells in the central portion of the culture chamber is eliminated within a time range of less than 1 day to 2.5 days,

depending on the proximity of the cells to the exit channels, thus meeting the specified requirements for maintaining physiological-like conditions within the chamber. However, the PDF has a long tail, extending beyond 4 days for the elimination of waste produced by cells near the walls of the culture chamber and in stagnant flow zones near the corners. This outcome is undesirable as it does not promote optimal cell proliferation and viability in these regions.

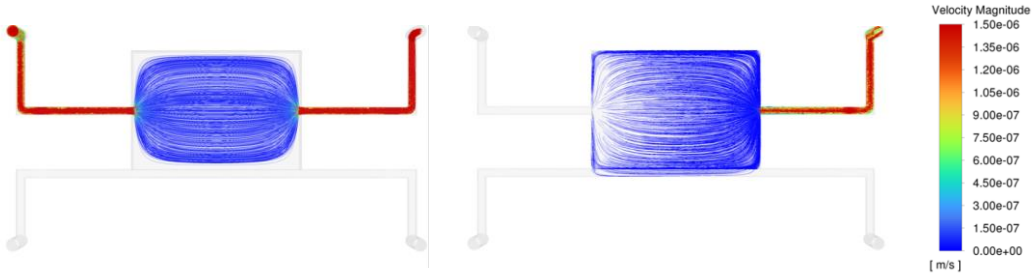

Figure 2: Trajectories of the nutrients supply (left) and waste elimination (right) for case 1

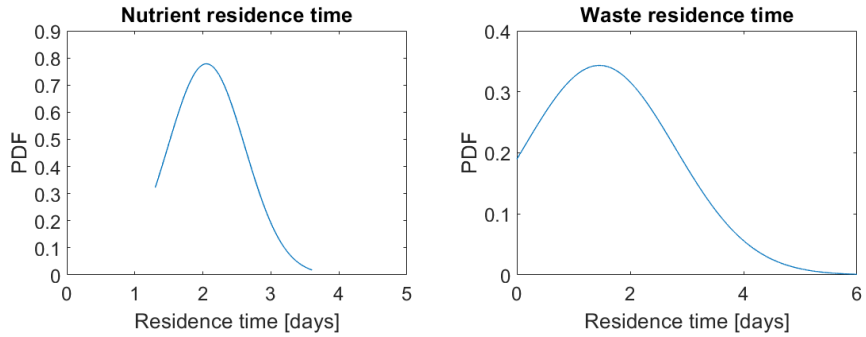

Figure 3: PDFs of the nutrient residence time (left) and waste elimination time (right) for case 1

The injection of drug substances into the chamber is achieved by setting a v_1/v_2 ratio of 1/10 (Case 1d). The results, in terms of drug perfusion trajectories within the culture chamber and PDFs of the drug residence time, are shown in Fig. 4. The drug can penetrate approximately 90% of the chamber volume. However, unlike the desired outcome, drug penetration is not homogeneous along the streamwise direction, as the front and rear portions of the cell culture chamber are less perfused compared to the central region. This is due to the drug stream's trajectory entering from the bottom-left corner of the chamber and exiting from the bottom-right corner. In terms of residence time, the 1-day requirement is met, with variability ranging from 0.5 to 2 days depending on how deeply the trajectories penetrate the chamber.

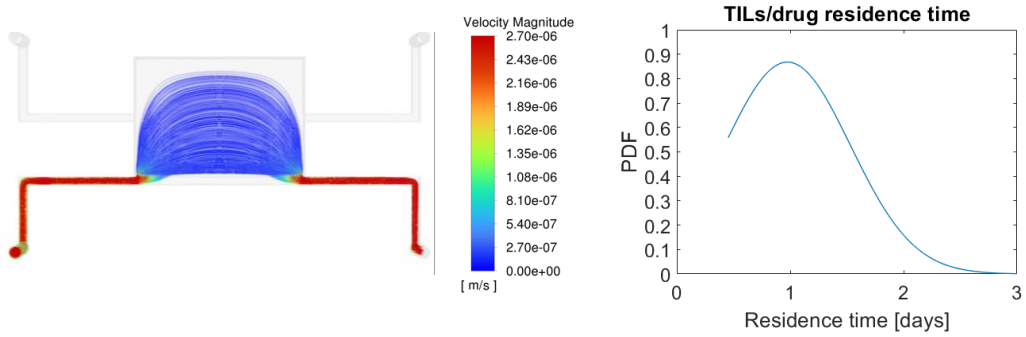

Figure 4: Trajectories of the drug perfusion in the culture chamber (left) and PDFs of the drug residence time (right) for case 1d

3.2 Analysis of the effect of the scaffold porosity

In this section, we investigate the effect of different scaffold porosity values within the range of 85%-95%, while keeping the averaged pore diameter constant at 100 μm.
When the scaffold is less porous, the flow lines entering from channel C_1 spread more widely in the cell culture chamber. Consequently, the nutrient supply trajectories reach all the cells more effectively, reducing stagnant flow regions near the corners of the chamber (Fig. 5). The residence time of nutrients slightly increases, while the variability of the PDF remains largely unchanged (left panel in Fig. 6). The opposite occurs when scaffold porosity increases.
Increasing the scaffold porosity to 95% has a detrimental effect on waste elimination as well as the increase of stagnant regions leads to a wider PDF compared to the 90% porosity case, resulting in a more variable PDF with waste elimination time reaching up to 6 days, which is incompatible with good cell viability. Conversely, the decrease of stagnant regions with a less porous scaffold has a beneficial effect on waste elimination (right panel in Fig.6).

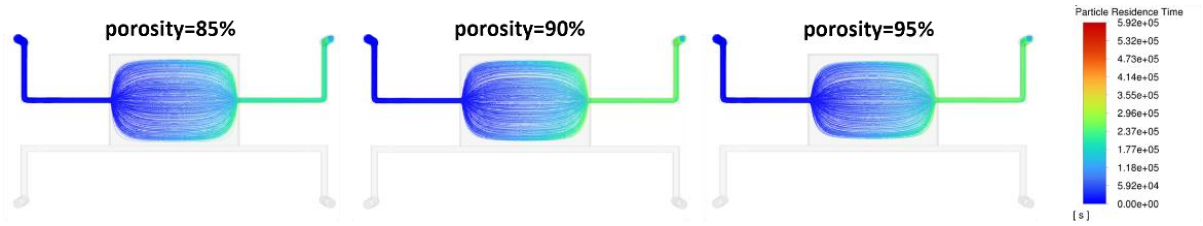

Figure 5: Effect of the scaffold porosity on the trajectories of the nutrient supply, colored by residence time. Comparison between cases 1, 2, and 3 (from left to right).

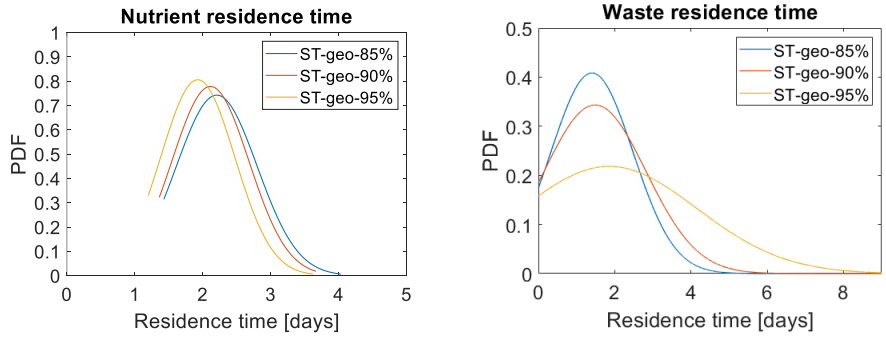

Figure 6: Effect of the scaffold porosity on the PDFs of the nutrient residence time (left) and waste elimination time (right). Comparison between cases 1, 2, and 3.

As for therapy perfusion, changes in scaffold porosity slightly affect the drug trajectories within the culture chamber (Fig. 7) and the associated residence time (Fig. 8). The effect is similar to what was observed for nutrient supply, with slightly improved drug penetration into the chamber and a marginally longer residence time.

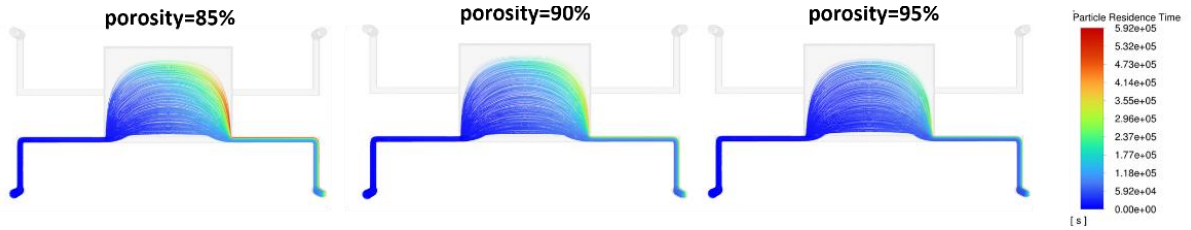

Figure 7: Effect of the scaffold porosity on the trajectories of the drug perfusion in the culture chamber, colored by residence time. Comparison between cases 1d, 2d, and 3d (from left to right).

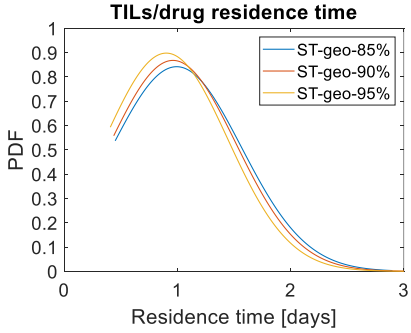

Figure 8: Effect of the scaffold porosity on the PDFs of the drug residence time. Comparison between cases 1d, 2d, and 3d.

3.3 Selection of the region of the culture chamber subjected to drug (through v_1/v_2 ratio)

In this section, we study the possible selection of the region of the culture chamber subjected to drug treatment by controlling the v_1/v_2 ratio. Figure 9 shows the drug perfusion trajectories within the cell culture chamber, colored by residence time, and the PDFs of drug residence time for cases 1d, 4d, and 5d. Setting $v_1=v_2$ allows treatment of half of the chamber. The only undesirable effect is the presence of two small, unperfused regions in the lower half of the chamber, in the foremost and rear parts, due to the shape of the drug trajectories. This setup is very useful for practical applications, as it facilitates direct comparison between treated and untreated cells within the same device, avoiding spurious effects from comparing two separate chips for treated and untreated cells. With $v_1=v_2$, the target residence time of 1 day is achieved with minimal variability in the PDF. This is also a favorable outcome, ensuring more homogeneous treatment conditions for all cells in the therapy-exposed part of the chamber.
On the other hand, setting $v_1=0$ allows the treatment of all the cells in the chamber. However, this configuration leads to increased variability in perfusion times due to the different trajectories of the drug substances. Therefore, a ratio of $v_1/v_2=1/10$ is recommended to minimize variability in residence times and ensure consistent, homogeneous perfusion of the cell culture chamber for optimal experimental reliability, in cases where treatment of all cells in the chamber is desired (noting that the upper 10% of the chamber remains untreated and should not be included in statistical studies).

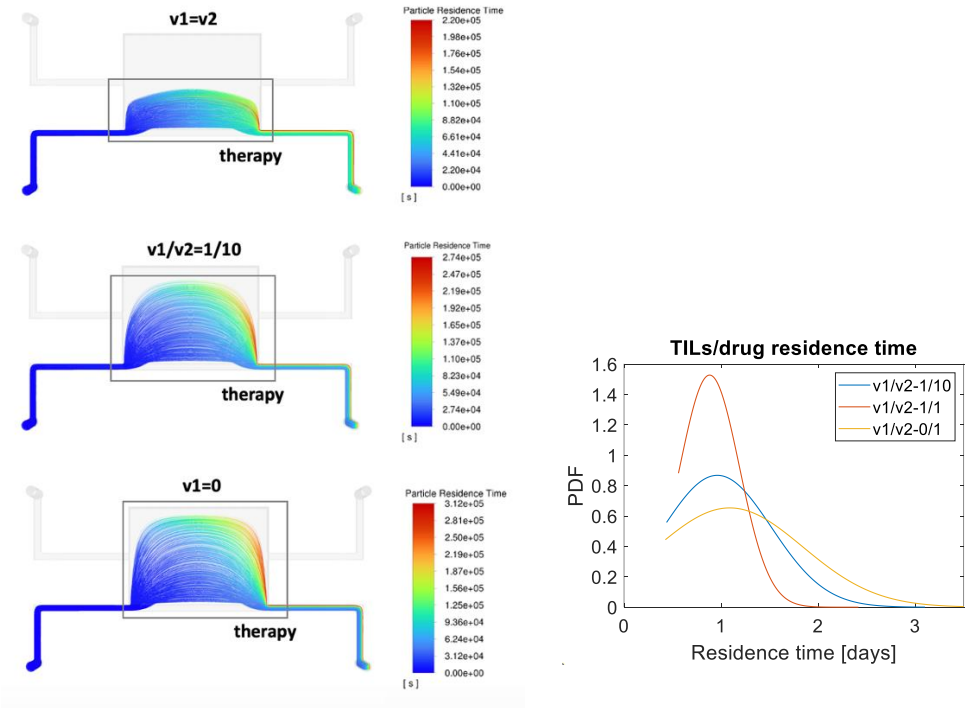

Figure 9: Effect of the v_1/v_2 ratio on the trajectories of the drug perfusion in the culture chamber, colored by residence time (left) and on the PDFs of the drug residence time (right). Comparison between cases 1d, 4d, and 5d.

4. CONCLUSION

In this study, CFD simulations were conducted to evaluate the performance of an organ-on-chip platform, ensuring optimal conditions for cell culture and therapy perfusion under controlled parameters. We analyzed flow patterns within the chip to determine whether they support efficient and time-regulated turnover of biological substances, thereby maximizing cell proliferation. These simulations demonstrate the potential of CFD as a predictive tool in selecting a dynamic microenvironment that promotes optimal cell viability.
We found that for scaffold porosity in the range of 85-90%, the requirements for nutrient supply, waste elimination, and drug treatments can be successfully met, even though with some variability among the cells. Furthermore, by precisely controlling the flow rates of the culture medium and therapeutic agents entering the organ-on-chip, it is possible to selectively target cells for treatment, enabling direct comparisons of the viability of treated and untreated cells on the same scaffold.
Future studies could focus on CFD-driven optimization of the device geometry to minimize variability in nutrient and drug residence times, as well as waste elimination time, with the aim of achieving uniform cell growth, proliferation, and expression. The goal is to replicate a dynamic microenvironment that closely mimics native tissue conditions, fostering cellular vitality and metabolic activity. Indeed, the combination of microfluidic technologies with computational simulations provides researchers with powerful tools for investigating complex biological systems and developing more effective therapeutic approaches.

Acknowledgments
The research leading to these results has received funding from the European Union – NextGenerationEU through the Italian Ministry of University and Research under PNRR – M4C2-I1.3 Project PE_00000019 "HEAL ITALIA", University of Pisa (CUP I53C22001440006). The views and opinions expressed are those of the authors only and do not necessarily reflect those of the European Union or the European Commission. Neither the European Union nor the European Commission can be held responsible for them

REFERENCES

[1] Bakuova, N.; Toktarkan, S.; Dyussembinov, D.; Azhibek, D.; Rakhymzhanov, A.; Kostas, K.; Kulsharova, G., “Design, Simulation, and Evaluation of Polymer-Based Microfluidic Devices via Computational Fluid Dynamics and Cell Culture On-Chip”, Biosensors, *13*, 754, 2023.

[2] Kimura, H.; Sakai, Y.; Fujii, T., “Organ/body-on-a-chip based on microfluidic technology for drug discovery”, Drug Metabolism and Pharmacokinetics, 33 (1), 43-48, 2018.

[3] Sheidaei, Z.; Akbarzadeh, P.; Kashaninejad, N., "Advances in numerical approaches for microfluidic cell analysis platforms", Journal of Science: Advanced Materials and Devices, 5 (3), 295-307, 2020.

[4] Jigar Panchal, H.; Kent, N.J.; Knox, A.J.S.; Harris, L.F., "Microfluidics in Haemostasis: A Review", Molecules, *25*, 833, 2020.

[5] Azizgolshani, H.; Coppeta, J.R.; Vedula E.M.; Marr, E.E.; Cain, B.P.; Luu, R.J.; Lech, M.P.; Kann, S.H.; et al., "High-throughput organ-on-chip platform with integrated programmable fluid flow and real-time sensing for complex tissue models in drug development workflows", Lab Chip, 21(8), 1454-1474, 2021.

[6] Sosa-Hernández, J.E.; Villalba-Rodríguez, A.M.; Romero-Castillo, K.D.; Aguilar-Aguila-Isaías, M.A.; García-Reyes, I.E.; Hernández-Antonio, A.; Ahmed, I.; Sharma, A.; Parra-Saldívar, R.; Iqbal, H.M.N., "Organs-on-a-Chip Module: A Review from the Development and Applications Perspective", Micromachines, 9, 536, 2018.

[7] Poon, C., "Measuring the density and viscosity of culture media for optimized computational fluid dynamics analysis of in vitro devices", Journal of the Mechanical Behavior of Biomedical Materials, 126, 105024, 2022.